

# Multi-scale Dynamics of Organic Light-Emitting Devices

A dissertation submitted to the faculty of the graduate school of the University of  
Minnesota

Kyle William Hershey

In partial fulfillment of the requirements for the degree of Doctor of Philosophy

Russell J. Holmes, Advisor

January 3, 2018

## Acknowledgements

I would like to thank my research advisor Russell J. Holmes for all of his guidance and advice.

Parents

Mary Beth

Dow Chemical for funding and collaboration. Dow scientists for research guidance, samples, etc.

# Dedication

To some people that I value

## Abstract

Over the last decade, organic light-emitting devices (OLEDs) have grown to receive tremendous attention for application in commercial displays and in lighting. While mostly successful for small format displays, challenges still exist that limit their performance for broader applications. Many of these limitations stem from a lack of understanding of charge and exciton dynamics and their impact on efficiency and stability. In this presentation, we describe novel device characterization and modelling efforts aimed at elucidating key dynamic processes in multiple regimes, including the microsecond transient behavior, steady-state, and long term degradation.

A model is presented which unifies both the transient and steady-state electroluminescence behavior of an OLED as a function of current density. The excellent agreement between the model and experiment enables a deeper understanding of efficiency reduction at high brightness. Additionally, the relatively ambiguous device efficiency parameter of charge balance is recast as an exciton formation efficiency. This framework permits a novel characterization paradigm for decoupling degradation pathways during OLED life-testing. In addition to the luminance loss, the degradation in emitter photoluminescence and exciton formation efficiency are also extracted. This technique is applied to an archetypical phosphorescent OLEDs, enabling more comprehensive design rules for device engineering to realize enhanced lifetime. Data science is a rising topic in industrial research. A system for enabling data science techniques within laboratory research is presented. Select useful applications are demonstrated.

# Contents

<b>1</b>	<b>Overview of Organic Semiconductors</b>	<b>6</b>
1.1	Organic Semiconductors . . . . .	6
1.2	Excitons . . . . .	6
1.2.1	Singlets and Triplets . . . . .	6
1.2.2	Electronic Transitions . . . . .	6
1.3	Charge Transport . . . . .	6
<b>2</b>	<b>Organic Light-Emitting Devices</b>	<b>7</b>
2.1	Fabrication Processes . . . . .	7
2.2	Characterization . . . . .	7
2.2.1	Luminance . . . . .	7
2.2.2	Efficiency Analysis . . . . .	7
2.3	Historical Development . . . . .	7
2.3.1	The First OLEDs . . . . .	7
2.3.2	Phosphorescence . . . . .	7
2.3.3	Host-Guest Systems . . . . .	7
2.3.4	Cohost Systems . . . . .	7
2.3.5	Thermally Activated Delayed Fluorescence . . . . .	7
2.4	Device Operation . . . . .	7
2.4.1	Dynamic Processes . . . . .	7
2.4.2	Efficiency Roll-Off . . . . .	7
<b>3</b>	<b>Transient and Steady-State Dynamics</b>	<b>8</b>
3.1	Motivation . . . . .	8
3.2	Theory . . . . .	8
3.2.1	Previous Efficiency Roll-Off Models . . . . .	8
3.3	Exciton Dynamics . . . . .	8
3.4	Polaron Dynamics . . . . .	8
3.5	Exciton Quenching in Photoluminescence . . . . .	8
3.5.1	Transient Electroluminescence . . . . .	9
3.5.2	Efficiency Analysis . . . . .	9
3.6	Experimental Details . . . . .	9
3.7	Application to Devices . . . . .	9
3.7.1	Overview of Approach . . . . .	9
3.7.2	Initializing Parameters with Quenching Only Steady-State Model . . . . .	9
3.7.3	Transient Modeling . . . . .	9
3.7.4	Term Efficiency During Transient . . . . .	10
3.7.5	Extracting Exciton Formation Efficiency . . . . .	10
3.7.6	Drift Model . . . . .	10
3.8	Understanding Assumptions of Polaron Model . . . . .	11
3.8.1	Carrier Injection . . . . .	11
3.8.2	Charge Imbalance . . . . .	11
<b>4</b>	<b>Integrated Photoluminescence Lifetimes</b>	<b>12</b>
4.1	Luminance as Efficiency Loss . . . . .	12
4.2	Photoluminescence Characterization . . . . .	12
4.2.1	Light Selection . . . . .	13
4.2.2	Absorption - Recombination Overlap . . . . .	13
4.2.3	Contact Degradation . . . . .	13
4.2.4	Quenching Changes During Degradation . . . . .	13

4.2.5	Verification with Excton Lifetime . . . . .	13
4.3	Experimental Implementation . . . . .	13
4.3.1	Hardware Setup . . . . .	13
4.3.2	Software Developement . . . . .	13
4.3.3	Database Integration . . . . .	13
<b>5</b>	<b>Applied Integrated Lifetimes</b>	<b>14</b>
5.1	CBP Host Thickness . . . . .	14
5.2	MEML Luminance Scaling . . . . .	14
5.3	Dow Cohost . . . . .	14
<b>6</b>	<b>Novel Blue Emitter Developement</b>	<b>15</b>
6.1	Molecular Systems . . . . .	15
6.2	Performance Optimization . . . . .	15
6.3	Solution Molecular Aggregation . . . . .	15
<b>7</b>	<b>Data Management for Devices</b>	<b>16</b>
<b>8</b>	<b>Modeling Out-Coupling</b>	<b>17</b>
8.1	Theory . . . . .	17
8.2	Recombination Zone Overlap During Lifetime . . . . .	17
<b>9</b>	<b>Future Research</b>	<b>18</b>
	<b>Bibliography</b>	<b>19</b>
	<b>Appendices</b>	<b>20</b>
<b>A</b>	<b>List of Publications</b>	<b>20</b>
<b>B</b>	<b>Out-Coupling Code</b>	<b>21</b>
<b>C</b>	<b>Lifetime Box Code</b>	<b>22</b>
<b>D</b>	<b>List of Figures</b>	<b>23</b>
<b>E</b>	<b>List of Tables</b>	<b>25</b>

# 1 Overview of Organic Semiconductors

## 1.1 Organic Semiconductors

## 1.2 Excitons

### 1.2.1 Singlets and Triplets

### 1.2.2 Electronic Transitions

## 1.3 Charge Transport

## **2 Organic Light-Emitting Devices**

### **2.1 Fabrication Processes**

### **2.2 Characterization**

#### **2.2.1 Luminance**

#### **2.2.2 Efficiency Analysis**

### **2.3 Historical Development**

#### **2.3.1 The First OLEDs**

#### **2.3.2 Phosphorescence**

#### **2.3.3 Host-Guest Systems**

#### **2.3.4 Cohost Systems**

#### **2.3.5 Thermally Activated Delayed Fluorescence**

### **2.4 Device Operation**

#### **2.4.1 Dynamic Processes**

#### **2.4.2 Efficiency Roll-Off**



### 3 Transient and Steady-State Dynamics

This section is referencing my paper.[2, 3]

#### 3.1 Motivation

#### 3.2 Theory

##### 3.2.1 Previous Efficiency Roll-Off Models

#### 3.3 Exciton Dynamics

$$\frac{dn_{ex}}{dt} = -\frac{n_{ex}}{\tau} - \frac{1}{2}k_{TT}n_{ex}^2 - k_{TP}n_{pol}n_{ex} + G_{ex} \quad (1)$$

$$G_{ex} = \frac{k_F}{4}n_{pol}^2 \quad (2)$$

#### 3.4 Polaron Dynamics

$$\frac{dn_{pol}}{dt} = \frac{-k_F}{2}n_{pol}^2 - \frac{n_{pol}}{\tau_l} + G_{pol} \quad (3)$$

#### 3.5 Exciton Quenching in Photoluminescence

$$V = \left[ \frac{J}{e\mu N_C} d^{2l+} \left( \frac{eN_0 k_B T_t}{\epsilon} \right)^l \right]^{\frac{1}{l+1}} = C J^{\frac{1}{l+1}} \quad (4)$$

$$n_{pol} = eN_c \left( \frac{\epsilon V}{ed^2 N_0 k T_t} \right)^l \quad (5)$$

$$\frac{L(n_{pol})}{L_0} = \frac{1}{1 + \tau k_{TP} n_{pol}} \quad (6)$$

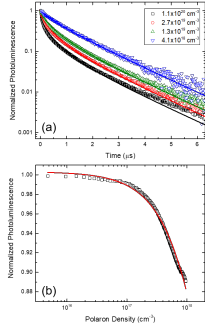


Figure 1: (a) Transient photoluminescence (PL) decays for several initial exciton densities with fits shown as solid lines using Eqn. 2. Fit parameters are discussed in SECTION. Exciton densities are calculated using measured incident power and beam size in combination iwht Beer's Law. (b) Steady-state PL quenching as a function of polaron density and the resulting fit from Eqn. 6 shown as the solid line.

### 3.5.1 Transient Electroluminescence

### 3.5.2 Efficiency Analysis

$$\eta_{EQE} = \eta_{OC}\eta_{PLX}\eta_{EF} \quad (7)$$

$$\eta_{EQE} = \frac{\eta_{OC}\eta_{ex}k_r}{G_{pol}/2} \quad (8)$$

$$\eta_{EF} = \frac{\frac{1}{2}k_F n_{pol}}{G_{pol}} = \frac{\frac{1}{2}k_F n_{pol}}{\frac{1}{2}k_F n_{pol} + \frac{1}{\tau_l}} \quad (9)$$

## 3.6 Experimental Details

### 3.7 Application to Devices

#### 3.7.1 Overview of Approach

#### 3.7.2 Initializing Parameters with Quenching Only Steady-State Model

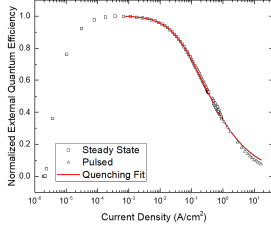


Figure 2: Normalized experimental  $\eta_{EQE}$  as a function of current density. Solid line is a fit to the data using Eqn. 1 and 3 in the absence of polaron loss. Pulsed  $\eta_{EQE}$  measurements are conducted using low duty cycle pulses to steady-state luminance to reduce Joule heating in device.

#### 3.7.3 Transient Modeling

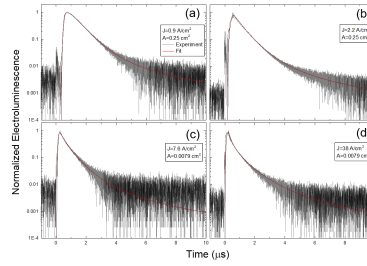


Figure 3: Transient electroluminescence (EL) for four different current densities (J) and device areas (A). (a) 0.25  $cm^2$  device at a current density during the pulse of  $J = 0.9 A/cm^2$  (b) 0.25  $cm^2$  device at  $J = 2.2 A/cm^2$  (c) 0.0079  $cm^2$  device at  $J = 7.6 A/cm^2$  (d) 0.0079  $cm^2$  device at  $J = 38 A/cm^2$

**Table 1: Fit parameter extracted from transient and steady state electroluminescence.**  
 Transient EL fit parameters averaged over all measured current densities.  $\eta_{EQE}$  Roll-off parameters averaged over several measured devices. Triple-exciton annihilation and triplet-polaron quenching rates are fixed to those obtained from fitting the normalized efficiency roll-off.

	Transient EL	Efficiency Roll-off
$\tau$ (s)	$6.9 \pm 0.1 \times 10^{-7}$	$6.1 \times 10^{-7}$
$k_{22}$ ( $\text{cm}^2/\text{s}$ )	$7.1 \times 10^{-12}$	$7.1 \times 10^{-12}$
$k_{32}$ ( $\text{cm}^2/\text{s}$ )	$3.3 \times 10^{-13}$	$3.3 \times 10^{-13}$
$k_T$ ( $\text{cm}^2/\text{s}$ )	$7.7 \pm 3.5 \times 10^{-12}$	$1.6 \times 10^{-11}$

### 3.7.4 Term Efficiency During Transient

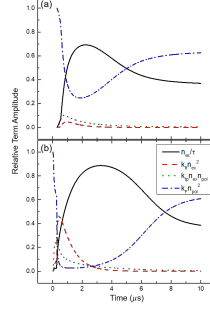


Figure 4: Term efficiency for each dynamical process influencing the exciton population for (a)  $0.25 \text{ cm}^2$  device operated at  $0.9 \text{ A/cm}^2$  for 500 ns and (b)  $0.785 \text{ mm}^2$  device operated at a current density of  $38 \text{ A/cm}^2$  for 250 ns. Relative term amplitude is calculated as the magnitude of each term in Eqn. 1 divided by the sum of absolute values of each term.

### 3.7.5 Extracting Exciton Formation Efficiency

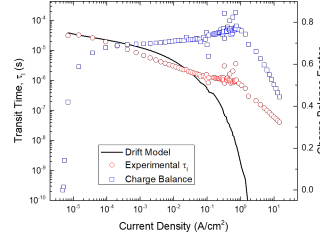


Figure 5: Transit time extracted from  $\eta_{EQE}$  measurements are shown as the red circles. Predictions using the drift model are calculated using Eqn. 10. The drift model assumes a uniform electric field. Good agreement between the experimental transit time and the drift model is found for a field distributed over 20 nm. The charge balance factor is shown as a function of current density in blue squares.

### 3.7.6 Drift Model

$$\tau_l = \frac{w}{E\mu(E)} \quad (10)$$

### 3.8 Understanding Assumptions of Polaron Model

#### 3.8.1 Carrier Injection

$$\frac{dn_h}{dt} = -k_F n_e n_h - \frac{n_h}{\tau_{lh}} + \frac{J_h}{ew} \quad (11)$$

$$\frac{dn_e}{dt} = -k_F n_e n_h - \frac{n_e}{\tau_{le}} + \frac{J_e}{ew} \quad (12)$$

$$J_1 \rightarrow J_h = J_2 \rightarrow J_e \quad (13)$$

$$\frac{J_e}{ew} + \frac{J_h}{ew} = \frac{J_1 + J_2}{ew} = \frac{2J}{ew} \quad (14)$$

$$J_1 = J_h \quad (15)$$

$$J_2 = J_e + J_l \quad (16)$$

$$J = J_h = J_e + J_l \quad (17)$$

$$G_{pol} - \frac{J_l}{ew} = \frac{2J - J_l}{ew} \quad (18)$$

#### 3.8.2 Charge Imbalance

$$\alpha = \frac{n_h}{n_e + n_h} \quad (19)$$

$$\left[ \frac{dn_{pol}}{dt} \right]_{formation} = -2k_F n_{pol}^2 \alpha (1 - \alpha) \quad (20)$$

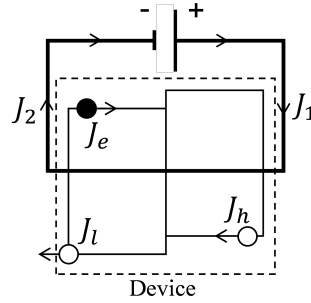


Figure 6: Current density formalism within the circuit. and are the currents measured on either side of the device. and are the electron and hole currents within the device and is the unbalanced current, assumed to be only holes, that leaks out of the opposing contact.

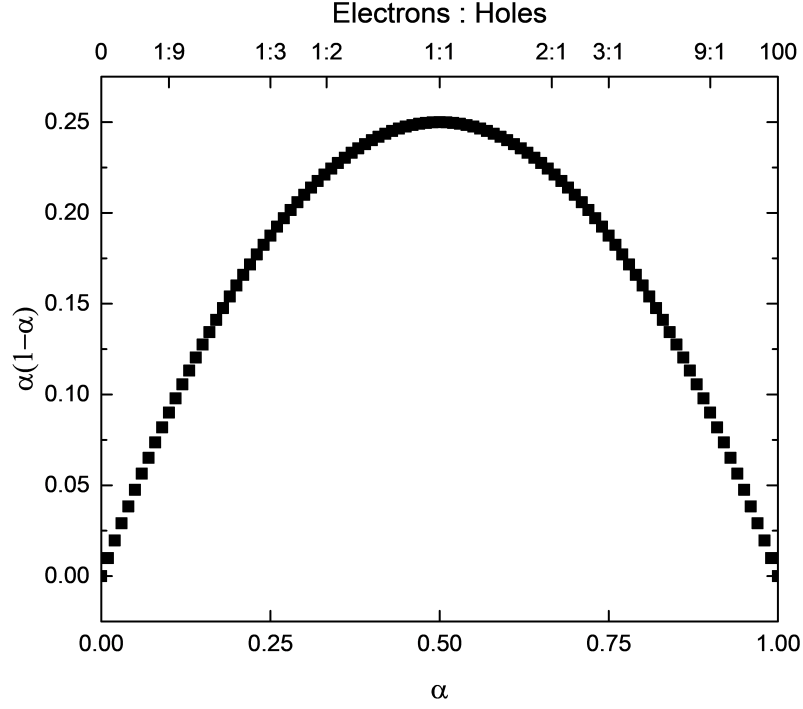


Figure 7: The quantity  $\alpha(1 - \alpha)$  is plotted as a function of the polaron composition,  $\alpha$  and the electron to hole ratio.

## 4 Integrated Photoluminescence Lifetimes

### 4.1 Luminance as Efficiency Loss

$$\eta_{EQE} = \eta_{PL}\eta_{OC}\chi\eta_{EF}\eta_{\tau} \quad (21)$$

$$\frac{\eta_{EQE}(t)}{\eta_{EQE}^0} = \frac{\eta_{PL}(t)}{\eta_{PL}^0} \frac{\eta_{EF}(t)}{\eta_{EF}^0} \quad (22)$$

### 4.2 Photoluminescence Characterization

$$\frac{\eta_{PL}(t)}{\eta_{PL}^0} = \frac{L_{PL}(t)}{L_{PL}^0} \frac{I^0}{I(t)} \quad (23)$$

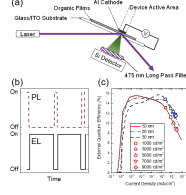


Figure 8: (a) Experimental configuration for the measurement of electro- (EL) and photoluminescence (PL) during OLED degradation. Laser excitation is incident on a subsection of the device area. The laser is aligned so that neither the incident nor reflected beam strikes the detector. Stray laser light is removed by a  $\lambda=475$  nm dielectric long pass filter. (b) Excitation scheme. EL and PL signals are probed independently with no temporal overlap. (c) External quantum efficiency versus current density and luminance for devices having emissive layer thickness of 10 nm, 20 nm and 30 nm.

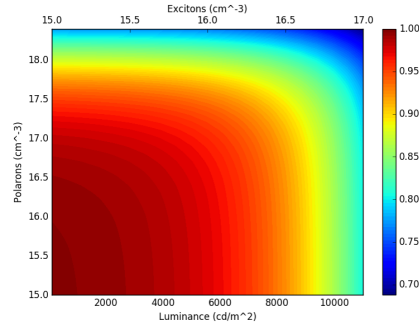


Figure 9: Multiplicative correction factor for exciton formation efficiency due to changes in quenching during lifetime. Shown as a function of polaron and exciton density as well as luminance, assuming a 10 nm emissive layer.

#### 4.2.1 Light Selection

#### 4.2.2 Absorption - Recombination Overlap

#### 4.2.3 Contact Degradation

#### 4.2.4 Quenching Changes During Degradation

#### 4.2.5 Verification with Excton Lifetime

### 4.3 Experimental Implementation

#### 4.3.1 Hardware Setup

#### 4.3.2 Software Developement

#### 4.3.3 Database Integration

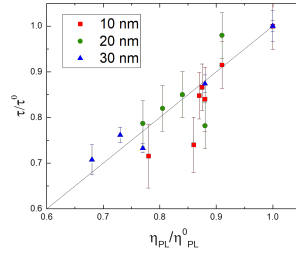


Figure 10: Exciton lifetime ratio extracted from transient PL measurements on degraded and undegraded devices as a function of emissive layer thickness.

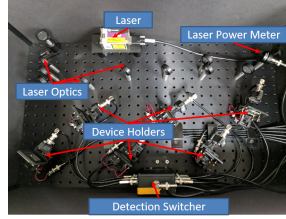


Figure 11: Device contacting, measurement, and optical hardware. Version 3 of the hardware is shown. Controlling hardware is shown in Fig. 12

## 5 Applied Integrated Lifetimes

### 5.1 CBP Host Thickness

### 5.2 MEML Luminance Scaling

### 5.3 Dow Cohost

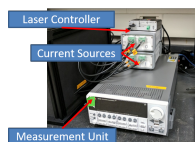


Figure 12: Source-Measure hardware and laser controller



Figure 13: 6 channel software controller. Selection of test type, laser control for alignment, and global settings are accessible on the top of the interface. Individual channel settings are grouped on the bottom.

## 6 Novel Blue Emitter Developement

### 6.1 Molecular Systems

### 6.2 Performance Optimization

### 6.3 Solution Molecular Aggregation



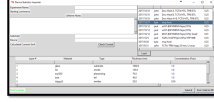


Figure 14: Test information for database import interface. The top left panel collects information about the specific device and lifetime. The right panel connects the device to a particular growth and architecture. The bottom panel confirms the architecture.

LiF/Al
Alq <sub>3</sub> – 30 nm
TPBi – 10 nm
CBP:Ir(ppy) <sub>3</sub> 6% – X nm
NPD – 30 nm
AQ1200
ITO

Figure 15: Device architecture, featuring EML thicknesses of X=10,20, and 30 nm

## 7 Data Management for Devices

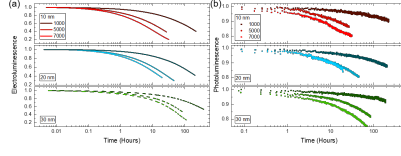


Figure 16: Device decay curves for multiple values of the initial luminance as a function of emissive layer thickness. Loss in (a) electroluminescence (EL) and (b) photoluminescence (PL) are shown and decrease monotonically with increasing luminance. For devices with a 10-nm-thick emissive layer, initial luminance values are  $1000 \text{ cd/m}^2$ ,  $5000 \text{ cd/m}^2$ , and  $7000 \text{ cd/m}^2$ . For devices with a 20-nm- or 30-nm-thick emissive layer, initial luminance values are  $1000 \text{ cd/m}^2$ ,  $5000 \text{ cd/m}^2$ , and  $7100 \text{ cd/m}^2$ .

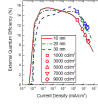


Figure 17: External Quantum Efficiency ( $\eta_{EQE}$ ) for the three architectures. Operational points for lifetime are shown in symbols.

## 8 Modeling Out-Coupling

### 8.1 Theory

### 8.2 Recombination Zone Overlap During Lifetime

**Table 1: Summary of device lifetimes**  
For each device, the starting luminance ( $L_0$ ), current density ( $J$ ), starting voltage ( $V_0$ ) and time at which 50% of the initial luminance is reached are shown.

$d_{\text{PM}} \text{ (nm)}$	$L_0 \text{ (cd/m}^2\text{)}$	$J \text{ (mA/cm}^2\text{)}$	$V_0 \text{ (V)}$	$t_{50} \text{ (hours)}$
10	1000	2.2	4.2	139.0
	3000	7.2	5.1	39.9
	5000	13.6	5.4	15.8
	7000	14.4	6.2	6.9
	9000	28.0	6.3	5.3
20	1000	2.2	5.4	141.1
	3000	7.2	6.0	33.1
	5000	12.4	7.2	17.2
	7100	19.2	7.3	10.0
	9000	24.0	7.5	8.0
30	1000	2.2	5.9	474
	5000	13.6	7.3	74.4
	7100	19.6	7.6	46
	8000	22.4	7.7	38.1

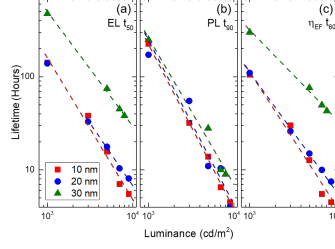


Figure 18: Extracted lifetimes for all 3 architectures as a function of luminance.

## 9 Future Research

## References

- [1] HERSHEY, K. W., AND COTTINGHAM, J. P. Material properties of pipes and reeds from the Southeast Asian khaen. *The Journal of the Acoustical Society of America* *129*, 4 (apr 2011), 2520–2520.
- [2] HERSHEY, K. W., AND HOLMES, R. J. Unified analysis of transient and steady-state electrophosphorescence using exciton and polaron dynamics modeling. *Journal of Applied Physics* *120*, 19 (2016), 195501.
- [3] HERSHEY, K. W., SUDDARD-BANGSUND, J., QIAN, G., AND HOLMES, R. J. Decoupling degradation in exciton formation and recombination during lifetime testing of organic light-emitting devices. *Applied Physics Letters* *111*, 11 (2017), 113301.
- [4] XU, F., HERSHEY, K. W., HOLMES, R. J., AND HOYE, T. R. Blue-Emitting Arylalkynyl Naphthalene Derivatives via a Hexadehydro-Diels-Alder Cascade Reaction. *Journal of the American Chemical Society* *138*, 39 (oct 2016), 12739–12742.

# Appendices

## A List of Publications

- HERSHEY, K. W., AND COTTINGHAM, J. P. Material properties of pipes and reeds from the Southeast Asian khaen. *The Journal of the Acoustical Society of America* 129, 4 (apr 2011), 2520–2520
- HERSHEY, K. W., AND HOLMES, R. J. Unified analysis of transient and steady-state electrophosphorescence using exciton and polaron dynamics modeling. *Journal of Applied Physics* 120, 19 (2016), 195501
- HERSHEY, K. W., SUDDARD-BANGSUND, J., QIAN, G., AND HOLMES, R. J. Decoupling degradation in exciton formation and recombination during lifetime testing of organic light-emitting devices. *Applied Physics Letters* 111, 11 (2017), 113301
- XU, F., HERSHEY, K. W., HOLMES, R. J., AND HOYE, T. R. Blue-Emitting Arylalkynyl Naphthalene Derivatives via a Hexadehydro-Diels-Alder Cascade Reaction. *Journal of the American Chemical Society* 138, 39 (oct 2016), 12739–12742

## B Out-Coupling Code

## C Lifetime Box Code

## D List of Figures

### List of Figures

1	(a) Transient photoluminescence (PL) decays for several initial exciton densities with fits shown as solid lines using Eqn. 2. Fit parameters are discussed in SECTION. Exciton densities are calculated using measured incident power and beam size in combination with Beer's Law. (b) Steady-state PL quenching as a function of polaron density and the resulting fit from Eqn. 6 shown as the solid line. . . . .	8
2	Normalized experimental $\eta_{EQE}$ as a function of current density. Solid line is a fit to the data using Eqn. 1 and 3 in the absence of polaron loss. Pulsed $\eta_{EQE}$ measurements are conducted using low duty cycle pulses to steady-state luminance to reduce Joule heating in device. . . .	9
3	Transient electroluminescence (EL) for four different current densities (J) and device areas (A). (a) $0.25 \text{ cm}^2$ device at a current density during the pulse of $J = 0.9 \text{ A/cm}^2$ (b) $0.25 \text{ cm}^2$ device at $J = 2.2 \text{ A/cm}^2$ (c) $0.0079 \text{ cm}^2$ device at $J = 7.6 \text{ A/cm}^2$ (d) $0.0079 \text{ cm}^2$ device at $J = 38 \text{ A/cm}^2$ . . . . .	9
4	Term efficiency for each dynamical process influencing the exciton population for (a) $0.25 \text{ cm}^2$ device operated at $0.9 \text{ A/cm}^2$ for 500 ns and (b) $0.785 \text{ mm}^2$ device operated at a current density of $38 \text{ A/cm}^2$ for 250 ns. Relative term amplitude is calculated as the magnitude of each term in Eqn. 1 divided by the sum of absolute values of each term. . . . .	10
5	Transit time extracted from $\eta_{EQE}$ measurements are shown as the red circles. Predictions using the drift model are calculated using Eqn. 10. The drift model assumes a uniform electric field. Good agreement between the experimental transit time and the drift model is found for a field distributed over 20 nm. The charge balance factor is shown as a function of current density in blue squares. . . . .	10
6	Current density formalism within the circuit. and are the currents measured on either side of the device. and are the electron and hole currents within the device and is the unbalanced current, assumed to be only holes, that leaks out of the opposing contact. . . . .	11
7	The quantity $\alpha(1 - \alpha)$ is plotted as a function of the polaron composition, $\alpha$ and the electron to hole ratio. . . . .	12
8	(a) Experimental configuration for the measurement of electro- (EL) and photoluminescence (PL) during OLED degradation. Laser excitation is incident on a subsection of the device area. The laser is aligned so that neither the incident nor reflected beam strikes the detector. Stray laser light is removed by a $\lambda=475 \text{ nm}$ dielectric long pass filter. (b) Excitation scheme. EL and PL signals are probed independently with no temporal overlap. (c) External quantum efficiency versus current density and luminance for devices having emissive layer thickness of 10 nm, 20 nm and 30 nm. . . . .	13
9	Multiplicative correction factor for exciton formation efficiency due to changes in quenching during lifetime. Shown as a function of polaron and exciton density as well as luminance, assuming a 10 nm emissive layer. . . . .	13
10	Exciton lifetime ratio extracted from transient PL measurements on degraded and undegraded devices as a function of emissive layer thickness. . . . .	14
11	Device contacting, measurement, and optical hardware. Version 3 of the hardware is shown. Controlling hardware is shown in Fig. 12 . . . . .	14
12	Source-Measure hardware and laser controller . . . . .	15
13	6 channel software controller. Selection of test type, laser control for alignment, and global settings are accessible on the top of the interface. Individual channel settings are grouped on the bottom. . . . .	15
14	Test information for database import interface. The top left panel collects information about the specific device and lifetime. The right panel connects the device to a particular growth and architecture. The bottom panel confirms the architecture. . . . .	16



15	Device architecture, featuring EML thicknesses of X=10,20, and 30 nm . . . . .	16
16	Device decay curves for multiple values of the initial luminance as a function of emissive layer thickness. Loss in (a) electroluminescence (EL) and (b) photoluminescence (PL) are shown and decrease monotonically with increasing luminance. For devices with a 10-nm-thick emissive layer, initial luminance values are 1000 $cd/m^2$ , 5000 $cd/m^2$ , and 7000 $cd/m^2$ . For devices with a 20-nm- or 30-nm-thick emissive layer, initial luminance values are 1000 $cd/m^2$ , 5000 $cd/m^2$ , and 7100 $cd/m^2$ . . . . .	17
17	External Quantum Efficiency ( $\eta_{EQE}$ ) for the three architectures. Operational points for lifetime are shown in symbols. . . . .	17
18	Extracted lifetimes for all 3 architectures as a function of luminance. . . . .	18

## **E List of Tables**

### **List of Tables**